

USING MINI-RADAR NETWORK FOR FLOOD FORECASTING IN MOLDOVA: HYDRORAD PROJECT

Valeriu CAZAC^{1*}

*John KALOGIROS*¹

*Marios ANAGNOSTOU*¹

*Frank MARZANO*²

*Juan STELLA*³

*Emmanouil ANAGNOSTOU*³

*Errico PICCIOTTI*²

*Giovanni CINQUE*²

*Mario MONTOPOLI*²

*Livio BERNARDINI*²

*Andrea VOLPI*⁴

*Andrea TELLESCHI*⁴

^{1*} *National Coordinator of HYDRORAD Project in Moldova*

¹ *National Observatory from Athens, Greece*

² *HIMET, High Innovation in Meteorology, L'Aquila, Italia*

³ *Civil and Environmental Engineering, University of Connecticut, Storrs, USA*

⁴ *ELDES, ELI International Company, Firenze, Italia*

1. Introduction

Rainfall estimates based on classical weather radar observations have quantitative limitations mainly due to the lack of uniqueness in the relationship of the single radar measurable (reflectivity) to the associated rainfall intensity. The polarization diversity capability of modern weather radars is expected to moderate this effect (Anagnostou et al. 2004). High-frequency/low-power polarization-diversity mini-radars can constitute a low-cost solution to the problem of hydrologic forecasting for urban and small-scale flood-prone basins and coastal areas not well covered by operational weather radar networks. Thus, short-wavelength radar systems (like X-band radars) became more attractive also for research purposes and they can either be mobile (trailer mounted, containerized or airborne) or static. Their

Informația expusă în acest articol este rezultatul implementării proiectului „HYDRORAD - Integrated advanced distributed system for hydro-meteorological monitoring and forecasting using low-cost high-performance X-band mini-radar and cellular network infrastructures” în cadrul programului de cercetare „7th Research Framework Programme (FP7), Research for SMEs”, finanțat de Uniunea Europeană și care atestă un studiu de caz în Republica Moldova.

Scopul principal al proiectului „HYDRORAD” a fost elaborarea și aplicarea sistemelor inovatoare de mini-radare cu dublă polarizare cu banda-X și a modelelor numerice de estimare a precipitațiilor, nowcasting, clasificarea precipitațiilor și integrarea cu modelele hidrologice și meteorologice pentru a fi utilizate în programele computerizate de analiză a vremii și prognozarea a inundațiilor.

Acest sistem de mini-radare este ușor de instalat și eficient de aplicat pentru arii restrânse și relief dezmembrat. Studiul de caz a început în luna august 2011 în Moldova, unde au fost efectuate cercetări în teren pentru testarea acestui sistem de mini-radare. În acest scop a fost instalată o rețea de trei mini-radare care în paralel efectuau scanări ale atmosferei cu un radar Doppler mobil polarimetric (tip XPOL) instalat în mijlocul rețelei.

Totodată, s-au efectuat măsurări ale precipitațiilor căzute, precum și măsurări video ale intensității ploii cu ajutorul aparatelor disdrometrice și pluviometre. Au fost aplicate algoritme polarimetrice originale pentru atenuarea corecției și estimarea precipitațiilor. Aceste rezultate au fost comparate cu datele de referință luate în câmp privind ploile convective și ploile moderate. Rezultatele au demonstrat că o astfel de rețea de mini-radare poate furniza informații de o precizie înaltă privind prognozarea precipitațiilor pe arii mici și cu relief dezmembrat și greu de scanat. Iar integrarea modelelor numerice meteorologice și hidrologice cu utilizarea informației on-line de la rețeaua de pluviometre oferă posibilitatea de a face predicții ale inundațiilor cu înaltă precizie.

limitations are the smaller range due to low power and the significant signal attenuation at X-band in heavy rain, which must be corrected because it introduces errors in the rainfall estimation.

The main objective of the HydroRad project was to develop an innovative dual-polarization X-band mini-radar system and software support tools for the use of weather and hydrologic applications. The overall system was tested in an experimental campaign where three mini-radar data and hydro-meteorological tool was tested against a state-of-the-art radar (XPOL) and in-situ weather stations (raingauges and disdrometer) measurements. The data were subsequently integrated to simulate the flood response for Bic basin.



Echipa HIDRORAD

2. Experimental Setup

The data used in this work were collected during Moldova Operational Field campaign (MOF) which took place in September and October 2011. The target area for the MOF campaign is the region around the Moldovan capital Chisinau. This region includes the basin of the river Bic with its tributaries and smaller rivers (Fig. 1). The terrain is characterized by low elevations up to 300 m.

The three mini-radars (Fig. 2) were installed in locations around Chisinau in order to cover the basin. XPol and the 2D-video disdrometer were installed in the center of mini-radars triangle in Chisinau in order to provide a reference basis for comparison

with the mini-radars. In addition six pairs of tipping raingauges were installed in different positions along the river (see Fig. 3 for their positions relative to XPol). The range of the radars was 60 km with a resolution of 120 m. Radar observations included the horizontal reflectivity Z_h , the differential reflectivity Z_{dr} and the differential phase Φ_{dp} , which is insensitive to radar calibration.

PPI scans at low elevation angles (up to 3.5°) were performed as well as RHI scans in selected azimuth angles in order to estimate the vertical structure of the rain field. The time period for a full volume scan was about 3 minutes. The disdrometer

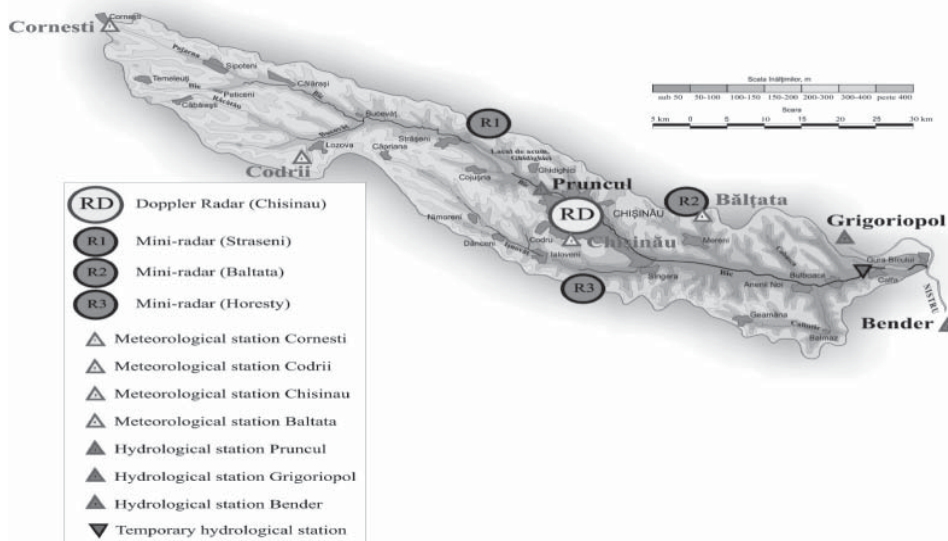


Fig. 1. The basin of the Bic river in central Moldova. The locations of the radars are shown.



Fig. 2. One of the mini-radars (left) and the XPol mobile radar with the nearby disdrometer and gauges (right)

data was used for the analysis of droplet size distribution, shape (axis ratio) and orientation of rain droplets, and the theoretical estimation (simulation) of polarimetric radar products.

3. Data Processing

At X-band frequencies attenuation of radar signal by rain can be quite significant and it can be larger than 10 dB in heavy rain. There are a number of rain attenuation correction algorithms like the ZPHI algorithm (Testud et al. 2000) used in this study, which is based on Φ_{DP} measurements, and its extension with the additions of a $\Phi_{DP} - Z_{DR}$ constraint (Bringi et al. 2001). The calibration of the reflectivity measurements of mini-radars was carried out by comparison with the radar products estimated from the disdrometer data (not shown here).

Rainfall rate R is estimated from radar measurements using polarimetric relations of rainfall parameters at X-band, which combine Z_h , Z_{dr} and specific differential phase K_{dp} , which is half the gradient of Φ_{dp} along the radar ray, as described in Matrosov

et al. (2002) and Park et al. (2005). In this study we evaluated three rainfall estimators. The first one is a classic Z-R estimator with steady coefficients which were evaluated from historic XPol data:

$$R = 3.36 \times 10^{-2} Z_h^{0.58}, \quad (1)$$

where R is in mm h^{-1} units and Z_h is in linear units instead of dBZ. The second estimation is a polarimetric estimator which is based the N_w normalization approach. Its constants were estimated from electromagnetic scattering simulations. N_w is the intercept parameter (units $\text{mm}^{-1} \text{m}^{-3}$) of rain droplet size distribution (DSD), which is approximated with a normalized Gamma distribution (Bringi and Chandrasekar 2001). N_w is obtained also from polarimetric relations found from the simulations. The polarimetric rainfall rate R estimator is:

$$R = 1.305 \times 10^{-3} N_w (Z_h / N_w)^{0.58}. \quad (2)$$

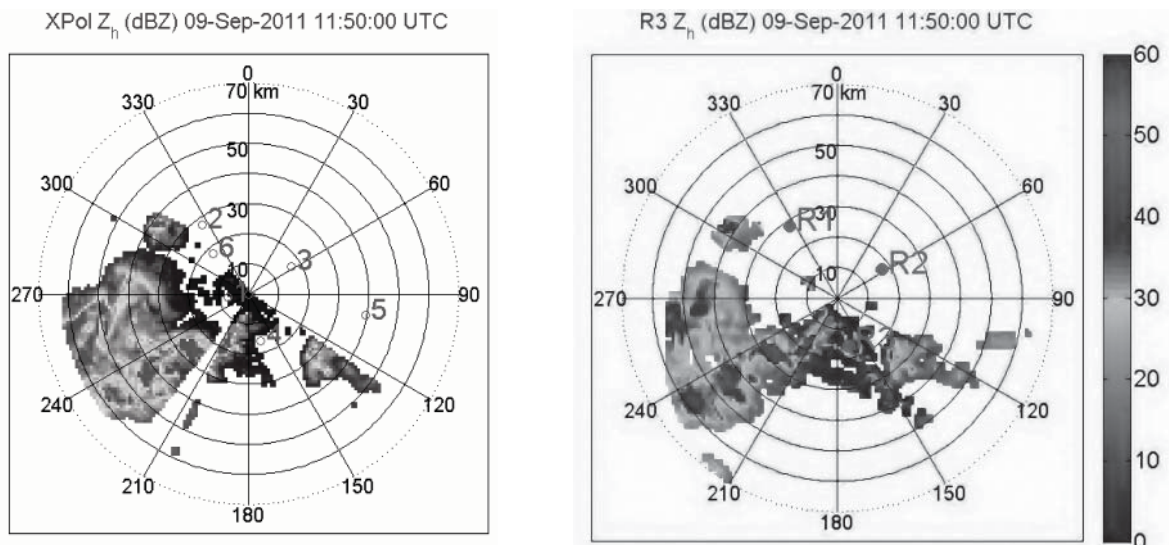


Fig. 3. A PPI of horizontal reflectivity Z_h measured from the XPol and the R3 mini-radar at an elevation angle of 1.5°. The locations of the three mini-radars and the six pairs of raingauges relative to XPol are also shown

The third rainfall estimator is a new polarimetric estimator which minimizes the approximation error using the theoretical Rayleigh scattering limit with the addition of a rational polynomial function of reflectivity-weighted droplet diameter to approximate the Mie character of scattering (Kalogiros et al. 2011):

$$R=0.8106F_R(\mu)N_w D_0^{4.67}f_R(D_0). \quad (3)$$

D_0 and μ are the median volume diameter and the shape parameter of the DSD, respectively, $d F_R$ is a function of μ , which is included in the Gamma approximation of the DSD, and f_R is a third degree rational polynomial of D_0 with constants evaluated by the simulations.

4. Results

Figure 3 shows an example of near simultaneous Z_h PPI from XPol and the R3 mini-radar. Both radars sense well convective rain cells coming from southwest. However, there are some differences which are due to the vertical profile of rain field and the different altitude of each volume of measure-

ments from the two radars which are separated by a distance of 16 km.

Figure 4 shows time series of comparison of accumulated rain in 30 minutes intervals from the two radars with raingauges. The polarimetric estimators Rp1 and Rp2 correspond to Eqs. (2) and (3), respectively, and follow well the raingauges reference measurements. The classic Z-R estimator shows lower values which is due to the fact that the constants in Eq. (1) were estimated from historic XPol data in Athens, Greece, where rain microphysics differ from Moldova region.

Figures 5 and 6 show the comparison of total accumulated rain in the experimental area from XPol and R3 mini-radar (classic and Rp2 estimators) during the rain event of 8-9 September 2011. The correlation coefficient is r , NB is the normalized bias and NSE in the normalized standard error. R3 rainfall estimates are similar with XPol but with a small overestimation by R3, which is probably due to errors in the calibration of the radars, and

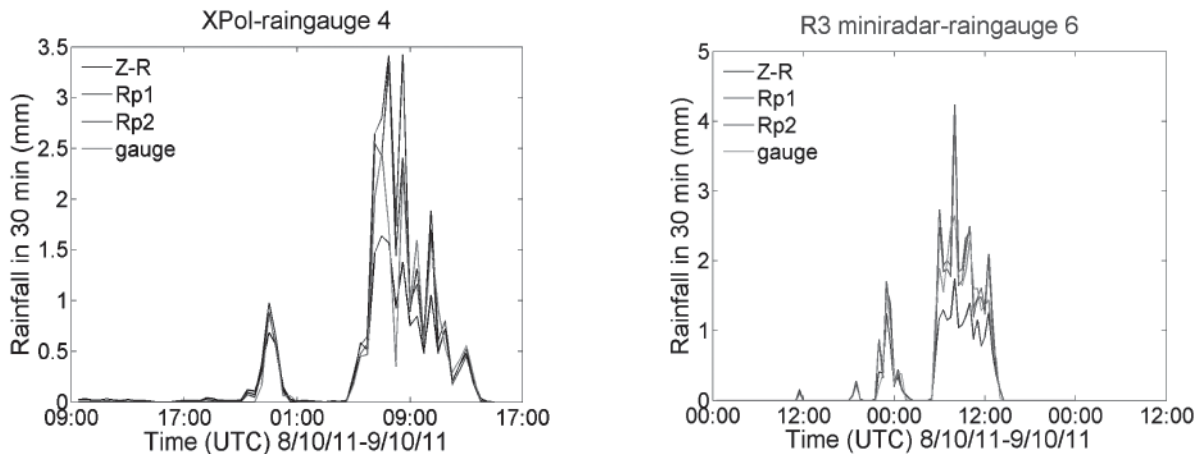


Fig. 4. Time series comparison of XPol and mini-radars rainfall estimators with raingauges.

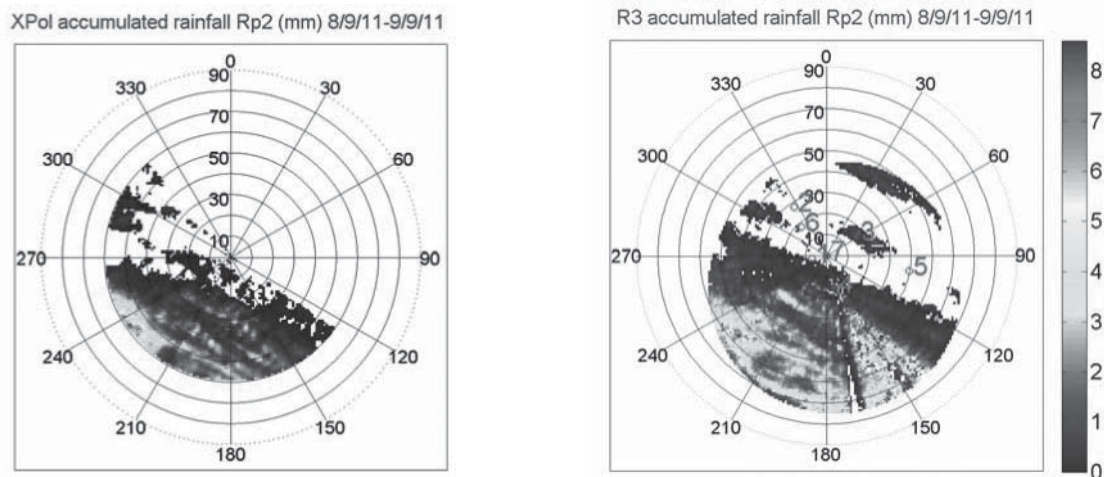


Fig. 5. PPI of total accumulated rain estimated using Eq. (3) from XPol and R3 in 8-9/9/2011.

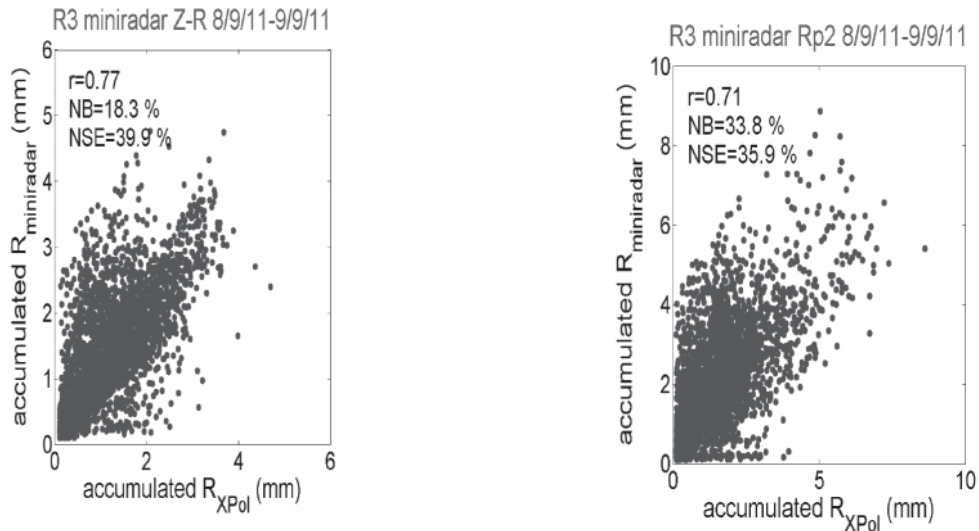


Fig. 6. Scatter plots of accumulated rain from XPol and R3 corresponding to Fig. 5.

significant scatter probably due to the differences in the time and altitude of the measurement volume of the two radars.

5. Hydrologic error analysis

In this section we present a case study of hydrologic model (HEC-HMS) integration based on data derived from the mini-radar network and quantitative precipitation forecasts from an operational numerical weather prediction model (MM5). The hydrologic modeling framework is used to characterize the uncertainty in flood prediction forced with the different (gauge versus mini radar network or forecasted rainfall) rainfall estimates. Specifically, rainfall fields interpolated by gauge (considered as our ground reference) and rainfall fields retrieved

by the network of the three mini radars will be used to force the hydrologic model for the targeted basin (Bic) in Moldova (see Fig. 1). Also rainfall forecasts from the MM5 atmospheric model tuned to Moldovan territory will be used to predict river flows.

Evaluation is based on qualitative time series plots of the hydrologic model simulated runoff using the mini-radar network rainfall estimates or forecasted rainfall and model simulated runoff using the reference gauge rainfall measurements. Specifically, to assess the hydrologic error propagation for the mini radar network we will perform the following hydrologic experiments:

- the hydrologic model is forced with rainfall from the rain gauge network to simulate the reference runoff;

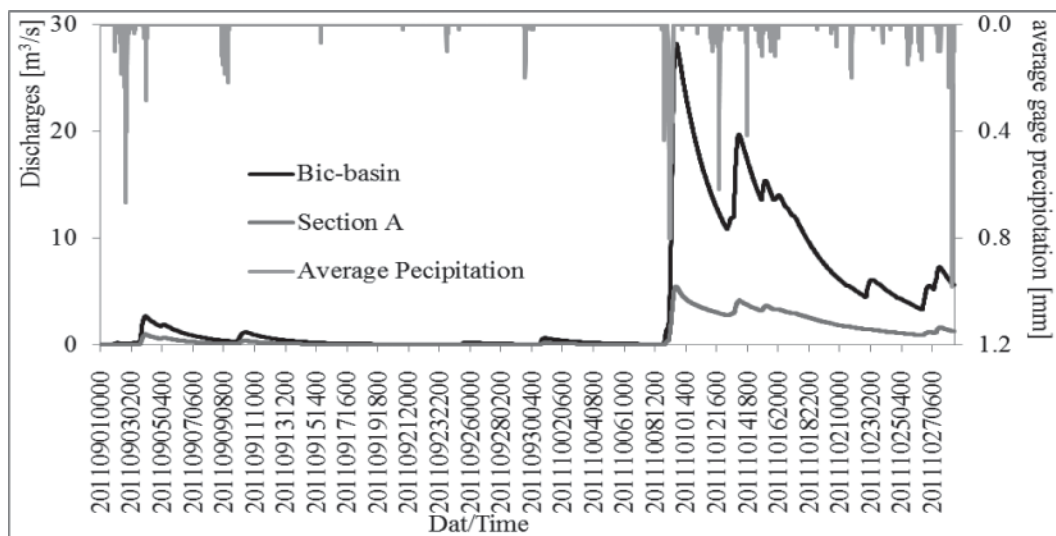


Fig. 7. Hydrologic model simulated runoff at the Bic basin outlet and an interior sub-basin based on rainfall measured by the rain gauge network

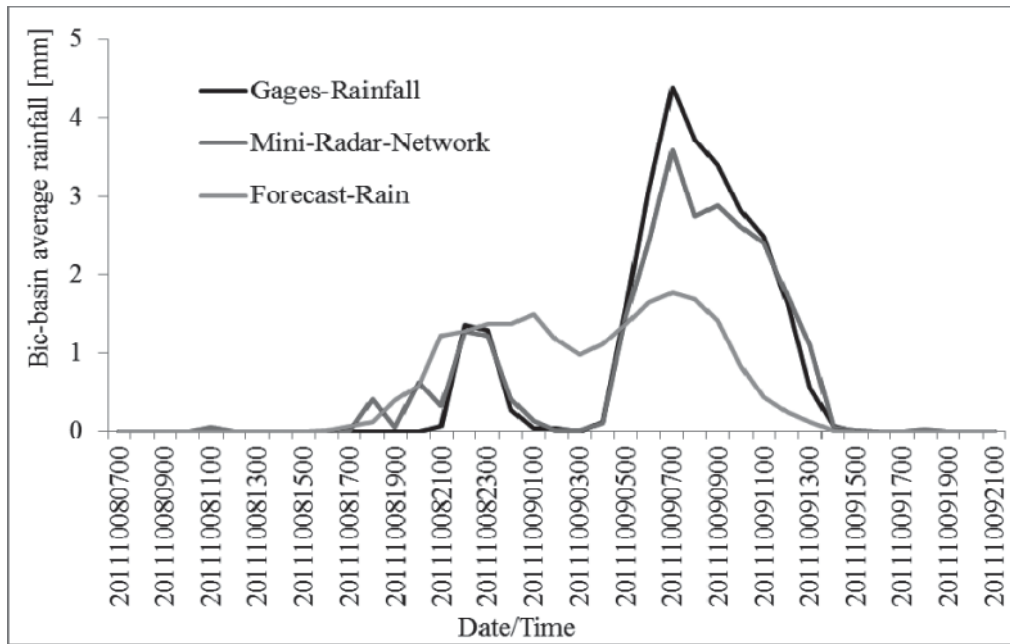


Fig. 8. Time series of Bic basin average rainfall rate based on gauge measurements, the mini-radar network estimates and the MM5 forecasted rainfall.

- the hydrologic model is forced with rainfall from the mini radar network at hourly time resolution and 1-km spatial resolution to simulate the radar-predicted runoff;
- the hydrologic model is forced with rainfall from MM5 atmospheric model rainfall forecasts to simulate forecasted runoff.

Comparisons of the above hydrologic model simulations will provide a qualitative indication of the use of mini radars in hydrologic prediction. In Figure 7 we show the basin average rainfall and the corresponding model predicted runoffs at Bic outlet and an interior basin downstream of a small reservoir during the period August-October 2011. The model simulations are based on the gauge rainfall data that can provide a continuous record of measured rainfall in the area. As indicated from the figure the period did not exhibited significant hydrologic events. The most significant event that produced notable basin response was in October 8-9 2011 that produced moderate peak runoff at the Bic basin outlet.

Furthermore, it is noted that during the October event all three mini radars were operational and provided continuous measurements of the storm event. Therefore, we will focus our hydrologic error propagation analysis in this single event and use all sub-basins that are within the distribution of the gauge network.

In Figure 8 we present the lower basin-avera-

ge rainfall time series retrieved by the mini-radar network, forecasted by MM5 and measured by the gauges. The general observation from the presented rainfall time series is the moderate underestimation (20%) and weaker temporal variability of basin average rainfall by the MM5 forecasts relative to gauges, which is not an unexpected outcome when it comes to quantitative precipitation forecasting of frontal systems. On the other hand the quantitative precipitation estimation by the mini-radar network observations exhibits close agreement with the gauge basin average rainfall. Specifically, the rainfall time series between the mini radar network and gauges are very well correlated (0.95), while the lower basin average mini radar network rainfall values exhibit a low underestimation (8%).

The corresponding flow predictions based on the various rainfall inputs is shown in Figure 9. A point to note is that the low basin average rainfall bias exhibited in Figure 8 is magnified through runoff simulations. The MM5 bias exhibits the most significant error propagation. This enhancement in underestimation is due to the dry initial basin conditions that resulted in a non-linear propagation of the basin response error from rainfall to runoff. Specifically, in the case of MM5 rainfall where rainfall rates were distributed over the basin with lower intensities, most of the rainfall was infiltrated causing an increase of the basin soil moisture and groundwater

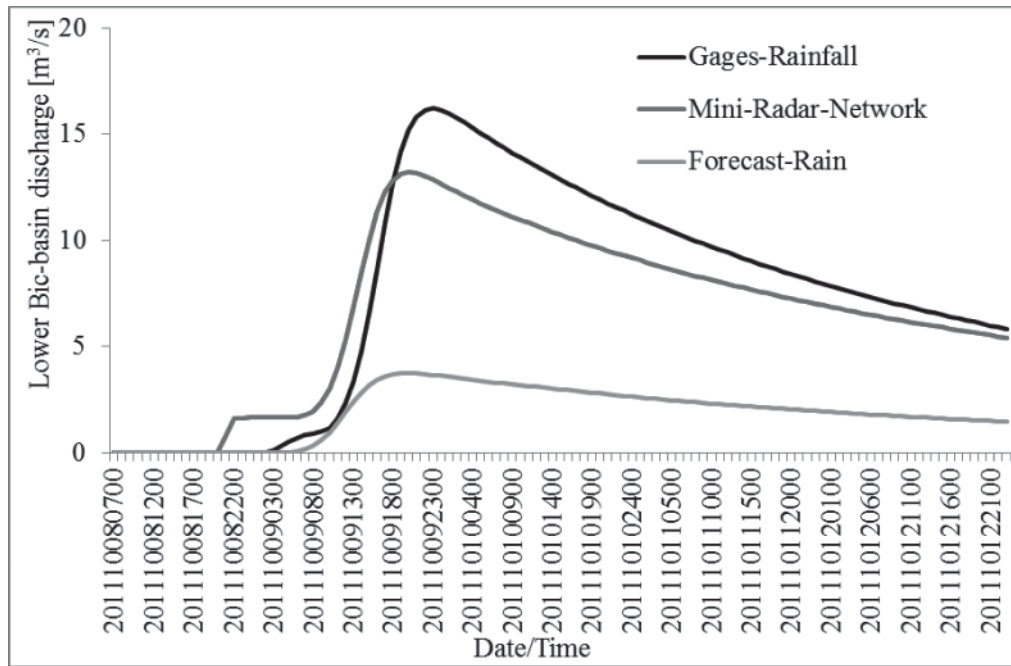


Fig. 9. Bic basin streamflow simulations from the hydrologic model forced with the various rainfall sources.

levels, and a significant increase in the bias of predicted basin runoff values between the MM5 rainfall and that derived from gauge interpolation. The error propagation in the mini-radar network rainfall estimates is lower than the in the MM5 rainfall, but, it still magnifies the rainfall bias to about 30% underestimation in runoff bias.

6. Conclusions

Weather and hydrologic hazards are at the top of environmental issues world-wide. X-band mini-radars are low cost mobile radar systems for weather and flood monitoring in small scales. Limitations in the operating characteristics of mini-radars (like the 3° wide beam-width compared to 1° of XPol) question the usefulness of their measurements. Our first results show that mini-radars can give reliable estimates of rainfall. Networks of mini-radars can cover broader areas in complex terrain where large expensive systems cannot achieve this. Furthermore, the hydrologic error propagation analysis showed that mini radar network rainfall estimates can be used to predict flows at various basin scales.

Acknowledgments

This work is part of the HYDRORAD project (Research for SMEs category–Grand agreement number FP7-SME-2008-1-232156) funded by EC 7th Framework Program.

References

1. Cazac V., Mihailescu C., Bejenaru G., Galca G.(2007). Apele de suprafata, „Știința”, Chișinău.
2. Anagnostou, E, Anagnostou M, Krajewski W, Kruger A, Miriovsky B (2004) High-resolution rainfall estimation from X-Band polarimetric radar measurements. *J. Hydrometeor.*, 5, 110–128.
3. Bringi V, Chandrasekar V (2001) Polarimetric Doppler weather radar. Cambridge University Press, Cambridge, UK.
4. Bringi V, Keenan T, Chandrasekar V (2001) Correcting C-band radar reflectivity and differential reflectivity data for rain attenuation: a self consistent method with constraints. *IEEE Trans. Geosci. Remote Sens.*, 39, 1906-1915.
5. Kalogiros J, Anagnostou M, Anagnostou E, Montopoli M, Picciotti E, Marzano FS (2011) Optimum estimation of rain microphysical parameters from polarimetric radar measurements. Submitted to the *IEEE Trans. Geosci. Remote Sens.*
6. Matrosov S, Clark K, Martner B, Tokay A (2002) X-band polarimetric radar measurements of rainfall. *J. Appl. Meteor.*, 41, 941-952.
7. Park S, Maki M, Iwanami K, Bringi V, Chandrasekar V (2005) Correction of radar reflectivity and differential reflectivity for rain attenuation at X-band, Part II: Evaluation and application. *J. Atmos. Ocean. Technol.*, 22, 1633-1655.
8. Testud J, Le Bouar E, Obligis E, Ali-Mehenni M (2000) The rain profiling algorithm applied to polarimetric weather radar. *J. Atmos. Ocean. Technol.*, 17, 332-356.